

Anal Bioanal Chem (2010) 398:1771–1780  
DOI 10.1007/s00216-010-4087-8

## ORIGINAL PAPER

# Development of an online p38 $\alpha$ mitogen-activated protein kinase binding assay and integration of LC–HR-MS

David Falck · Jon S. B. de Vlieger ·  
Wilfried M. A. Niessen · Jeroen Kool ·  
Maarten Honing · Martin Giera · Hubertus Irth

Received: 29 June 2010 / Revised: 28 July 2010 / Accepted: 2 August 2010 / Published online: 22 August 2010  
© The Author(s) 2010. This article is published with open access at [Springerlink.com](http://Springerlink.com)

**Abstract** A high-resolution screening method was developed for the p38 $\alpha$  mitogen-activated protein kinase to detect and identify small-molecule binders. Its central role in inflammatory diseases makes this enzyme a very important drug target. The setup integrates separation by high-performance liquid chromatography with two parallel detection techniques. High-resolution mass spectrometry gives structural information to identify small molecules while an online enzyme binding detection method provides data on p38 $\alpha$  binding. The separation step allows the individual assessment of compounds in a mixture and links affinity and structure information via the retention time. Enzyme binding detection was achieved with a competitive binding assay based on fluorescence enhancement which has a simple principle, is inexpensive, and is easy to interpret. The concentrations of p38 $\alpha$  and the fluorescence tracer SK&F86002 were optimized as well as incubation temperature, formic acid content of the LC eluents, and the material of the incubation tubing. The latter notably improved the screening of highly lipophilic compounds. For optimization and validation purposes, the known kinase inhibitors BIRB796, TAK715, and MAPK11 were used

among others. The result is a high-quality assay with  $Z'$  factors around 0.8, which is suitable for semi-quantitative affinity measurements and applicable to various binding modes. Furthermore, the integrated approach gives affinity data on individual compounds instead of averaged ones for mixtures.

**Keywords** p38 MAP kinase · High-resolution screening · Fluorescence enhancement · LC–MS · Bioassays

## Introduction

Kinases are certainly among the most important target classes in contemporary drug discovery [1]. The mitogen-activated protein (MAP) kinase p38 (p38) is one prominent example of a drug target kinase, especially its most important isoform p38 $\alpha$  [2, 3]. It is involved in signal transduction pathways, transmitting signals through successive activation by phosphorylation [4]. Being one of the important mediators for a cell's response to extracellular stimuli, this pathway presents a promising opportunity for drug intervention [5]. Because p38 $\alpha$  is heavily involved in inflammation processes, the envisaged diseases are mostly chronic inflammatory diseases like rheumatoid arthritis, psoriasis, or Crohn's disease [6]. Several p38 $\alpha$  inhibitors, which target these diseases, are currently in different stages of preclinical and clinical development up to phase II [3, 7]. Nearly all known kinase inhibitors show interactions with the highly conserved adenosine triphosphate (ATP)-binding pocket. Therefore, most early kinase inhibitors, possessing only these interactions, exhibited poor kinase selectivity [5]. Although different systems of categorization exist, these will be called type I inhibitors. Type I inhibitors used in this study are TAK715 [8], MAP kinase inhibitor 1

**Electronic supplementary material** The online version of this article (doi:10.1007/s00216-010-4087-8) contains supplementary material, which is available to authorized users.

D. Falck · J. S. B. de Vlieger · W. M. A. Niessen · J. Kool ·  
M. Giera (✉) · H. Irth  
LACDR-Division of Biomolecular Analysis,  
Department of Chemistry and Pharmaceutical Sciences,  
VU University Amsterdam,  
1081 HV Amsterdam, The Netherlands  
e-mail: [mgiera@few.vu.nl](mailto:mgiera@few.vu.nl)

M. Honing  
Department of Medicinal Chemistry, MSD Research Laboratories,  
5349 AB Oss, The Netherlands

(MAPK11) from Merck KGaA [9], and SK&F86002 (SKF) [9]. The discovery of an allosteric binding pocket adjacent to the ATP-binding site led to the discovery of inhibitors using both sites (type II). BIRB796 is a prominent example of this type of binding [10, 11]. Consequently, type III binders like 1-(3-*tert*-butyl-1-methyl-1*H*-pyrazol-5-yl)-3-(4-chlorophenyl)urea (pyrazolourea) are targeting only this allosteric site [12]. The type IV inhibitors are not binding to either of the two pockets, as has been discovered, e.g., for GNF-2 binding to the Bcr-abl kinase [13]. The importance of p38 $\alpha$  has led to a multitude of assay principles for the identification of small molecules targeting this kinase [14, 15]. Among the cell-free *in vitro* formats for p38 $\alpha$ , those based on activity and those based on affinity can be distinguished. As readout for activity-based methods, scintillation [11] and fluorescence polarization [16] have been used among others [14, 15]. These formats require expensive reagents (antibodies, etc.) and rely on labels which can impair the usefulness of results, or they involve handling radioactivity. In addition to these drawbacks, activity assays can, by definition, not employ the non-phosphorylated kinase as target. This is the advantage of affinity-based assays. However, scintillation [17], chemiluminescence [16], and fluorescence polarization [18] suffer from similar reagent-based drawbacks as mentioned above. Furthermore, some label-free technologies, like surface plasmon resonance [16] or isothermal titration calorimetry [19], have been employed, which avoid additional reagents and the problems of molecular probes. Still, these techniques are complex, and instrumental requirements and logistics may limit their throughput. A relatively simple approach was used by Pargellis et al. during the discovery of BIRB796 [10, 11]. The method is based on fluorescence enhancement and requires solely native p38 and the small molecule kinase inhibitor SKF. SKF shows fluorescence, which is strongly enhanced upon binding to the target enzyme. Therefore, high fluorescence intensity indicates a high concentration of the enzyme–tracer complex. A compound showing affinity to the target enzyme will compete with the tracer, thus reducing the concentration of enzyme–tracer complex and thereby reducing the fluorescence. This principle enables a competitive binding assay in a homogeneous setup, which is based on the strong difference in fluorescence intensity between the free tracer and the enzyme–tracer complex. Because of its convenience and the possibility to use non-phosphorylated p38 $\alpha$  as target, this technique presented a good basis for the development of a high-resolution screening (HRS) platform. HRS is defined by the combination of separation and screening in an integrated system. Therefore, it enables the affinity assessment and the simultaneous structural characterization of individual compounds in mixtures [20, 21]. This feature makes HRS platforms especially attractive when complex mixtures such

as metabolic incubations [22], combinatorial mixtures [21], or natural extracts [23] are screened where dereplication, affinity, and structural information are crucial. In contrast to conventional high-throughput screening (HTS), isolation of individual compounds not showing affinity can be avoided. Thus, the laborious development of high-yield synthesis and isolation methods can be limited to compounds showing the desired affinity. One common approach in HRS is the use of online post-column assays, which have been recently reviewed by Shi et al. [24]. Colorimetry-, fluorescence-, and mass-spectrometry-based readouts were developed in both homogeneous and inhomogeneous formats. Homogeneous setups are easier to apply, so their significance exceeds inhomogeneous setups in cases where background fluorescence is of minor importance. However, HRS formats described so far are either activity-based [21, 23] or target a receptor [20, 22]. We report the implementation of the enzyme p38 $\alpha$  as the first kinase to be targeted in an online post-column binding assay (HRS system). Furthermore, the screening of highly lipophilic molecules was greatly improved by the unprecedented use of covalently modified fused silica tubing as material for post-column incubation, resulting in improved affinity signals.

## Materials and methods

### Materials

Human recombinant p38 $\alpha$ , ORGX, BIRB796, and TAK715 were a kind gift of MSD Research Laboratories (Oss, the Netherlands). SKF and MAPK11 were purchased from Merck KGaA (Darmstadt, Germany). Enzyme-linked immunosorbent assay (ELISA) blocking reagent was delivered by Roche Diagnostics (Mannheim, Germany). Pyrazolourea was obtained from Ambinter (Paris, France). All other chemicals were from Sigma-Aldrich (Schnellendorf, Germany). Fused silica tubing (250- $\mu$ m inner and 375- $\mu$ m outer diameter) untreated or covalently coated with polyethylene glycol (PEG), methyl, or methyl/phenyl groups was also purchased from Sigma-Aldrich (Schnellendorf, Germany). Black polypropylene microtiter plates with ninety-six “flat”-bottom chimney wells from Greiner Bio-one (Alphen a/d Rijn, The Netherlands) were used. Methanol (liquid chromatography (LC)–mass spectrometry (MS) grade) and formic acid (ULC–MS grade) were obtained from Biosolve (Valkenswaard, the Netherlands). Purified water was generated with a Milli-Q academic from Millipore (Amsterdam, the Netherlands).

### Instrumentation

Ninety-six-well plate experiments were performed on a Victor3 plate reader from Perkin-Elmer (Groningen, the

Netherlands). The setup used for the online assay included two LC-20 AD and two LC-10 AD isocratic pumps, a SIL-20 AC autosampler, one CTO-20 AC and one CTO-10 AC column oven, an RF-10AXL fluorescence detector, a CBM-20A controller, and an ion trap time-of-flight (IT-TOF) mass spectrometer equipped with an ESI source, all products of Shimadzu ('s Hertogenbosch, the Netherlands). HR-MS spectra were obtained from  $m/z$  200 to 650, switching positive- and negative-ion mode with 10-ms accumulation time each. The curved desolvation line and the heating block were equilibrated at 200 °C and the voltages applied were 5 kV to the interface and 1.7 kV to the detector. Nitrogen (99.9990%) was used at flows of 1.5 and 10 L/min as nebulizing gas and drying gas, respectively. To allow accurate mass measurements, external calibration of the IT-TOF was performed using TFA clusters.

Furthermore, two superloops and two pulse dampeners made in-house were used.

#### Plate reader assay

A 20 mM Tris–HCl buffer (pH 7.5), containing 10 mM MgCl<sub>2</sub>, 2 g/L PEG 6000, and 0.2 g/L ELISA blocking reagent (Tris buffer), was used in all experiments. All solutions of p38 $\alpha$  were prepared in Tris buffer. Enzyme stock solutions were stored at –80 °C until use. During online experiments, the enzyme solutions were kept at 0 °C. A stock solution of SKF (2 mM) was made in dimethyl sulfoxide (DMSO) and further diluted with Tris buffer. Solutions of inhibitors were prepared in 1:1 water/methanol containing 0.01% formic acid from 2- to 5-mM stock solutions in methanol (DMSO in case of MAPK11). Small-molecule stock solutions were stored at –20 °C.

For plate reader measurements, the wells were filled with 50  $\mu$ L enzyme solution, 12.5  $\mu$ L inhibitor solution, and 50  $\mu$ L SKF solution in the given order. Fluorescence was

measured at 25 °C with the wavelength of absorption and emission being 355 $\pm$ 4 and 405 $\pm$ 5 nm, respectively. The sum of ten flashes was used as readout to improve performance. Saturation of a 90-nM solution of p38 $\alpha$  with SKF was determined by using a concentration range from 40 to 2,500 nM of SKF. The  $Z'$  factor is a measure for assay quality. If not otherwise stated, it was calculated according to the original publication of Zhang et al. [25]. A more detailed explanation is given in the “Results and discussion” section. Measurements of the  $Z'$  factor dependence on enzyme concentration were performed on 3 days with five repeats per day and a final concentration of 3  $\mu$ M SKF. For full inhibition, TAK715 was added to a final concentration of 1  $\mu$ M, while the control values contained only the corresponding amount (see above) of high-performance liquid chromatography (HPLC) solvents.

#### Online assay

HPLC solvents were 100:1 water/methanol (solvent A) and 100:1 methanol/water (solvent B), both containing 0.01% formic acid. The instrumental setup described by de Vlieger et al. [20] was used for the analysis, with one enzyme binding detection line and the following modifications (cf Fig. 1). HPLC was done either in flow injection analysis (FIA) mode (where no separation column is present) or with a SunFire C18 column 30 $\times$ 2.1 mm, 3.5- $\mu$ m particles (Waters, Milford, MA, USA; Fig. 1, 2). Ten microliters of the sample was injected (Fig. 1, 1) into a flow of 113  $\mu$ L/min. Elution was performed at 40 °C, either isocratic at different methanol concentrations or using a binary gradient. Post-column, the flow was split 1:9 (Fig. 1, 3), sending 100  $\mu$ L/min to high-resolution mass spectrometry (HR-MS) detection and 13  $\mu$ L/min to the enzyme binding detection. To the 13  $\mu$ L/min HPLC eluent, first 50  $\mu$ L/min of a 200 nM p38 $\alpha$  solution was added (Fig. 1, 4) and thereafter 50  $\mu$ L/min of a 1,400-nM solution of SKF (Fig. 1, 6).

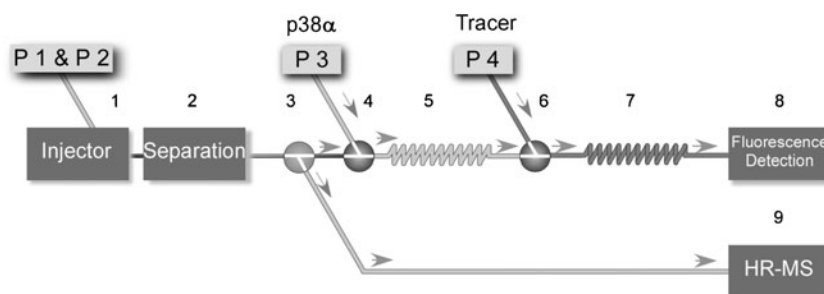


**Fig. 1** Scheme of the online setup. The system enables the separation of mixtures and subsequent parallel detection of enzyme binding and accurate mass. The samples are injected (1) into and separated (2) by an HPLC system. The eluent is split (3) between HR-MS and enzyme binding detection. The fraction which enters the enzyme binding detection is mixed with the target (4) and the tracer (6) and incubated

after each mixing step, 24 s for the target–ligand interaction (5) and 11 s for the target–tracer interaction (7). Finally, the fluorescence is measured (8) as readout of affinity towards p38 $\alpha$ . In parallel, the second part of the eluent is analyzed by HR-MS (9), delivering structural information to identify the small molecules tested

These solutions were constantly released by a linear setup of an LC-10 AD pump, a pulse dampener with restriction capillary, and a superloop each. Following each addition, the mixture was incubated in PEG-deactivated fused silica loops of 25  $\mu\text{L}$  (Fig. 1, 5) and 20  $\mu\text{L}$  (Fig. 1, 7), respectively. The incubation loops were kept at 25  $^{\circ}\text{C}$  in a second column oven. The resulting incubation times were 24 s for the target–ligand interaction (Fig. 1, 5) and 11 s for the target–tracer interaction (Fig. 1, 7). Finally, at concentrations of 90 nM p38 $\alpha$  and 630 nM of SKF, the fluorescence was measured with excitation at  $355\pm 7.5$  nm and emission at  $425\pm 7.5$  nm (Fig. 1, 8). The used detector settings were gain 4, recorder range 1, and sensitivity medium.

The influence of the methanol concentration on the maximum signal was assessed in two consecutive measurements. To this end, a stepwise gradient was used starting at 100% A and increasing the fraction of B by 15% approximately every 10 min. In the first run, the baseline without inhibition was recorded. In the second run, MAPK11 was added to the SKF solution for full inhibition, reaching a final assay concentration of around 0.9  $\mu\text{M}$ . By comparing these measurements, the assay window in relation to the different organic modifier concentrations can be estimated.

In order to assess the influence of the incubation tubing material, two measurements were carried out, in which the volume and therefore the incubation time were kept constant: in the first experiment, polyether ether ketone (PEEK) of 250- $\mu\text{m}$  and 170- $\mu\text{m}$  inner diameter (ID), polytetrafluoroethylene (PTFE) of 250- $\mu\text{m}$  ID, and untreated fused silica of 250- $\mu\text{m}$  ID were compared by injecting a 2- $\mu\text{M}$  solution of ORGX in FIA mode at 60% B. In a second experiment, 250- $\mu\text{m}$  ID fused silica tubings with covalent coatings of different polarity were compared. In these experiments, a 20- $\mu\text{M}$  solution of ORGX was injected in FIA mode at 60% B. The coatings were PEG (polar), a mixture of phenyl and methyl groups (intermediate), or methyl groups only (non-polar).

The online  $Z'$  factor was calculated from triplicate injections each of a control (blank) experiment and a full inhibition sample on five different days. The full inhibition sample was a mixture of 50  $\mu\text{M}$  BIRB796, 20  $\mu\text{M}$  ORGX, and 20  $\mu\text{M}$  TAK715 while the control sample was a 1:1 mixture of the solvents. The separation was carried out with the following gradient: 0 to 1.0 min isocratic at 50% B, 1.0 to 12.5 min linear to 90% B, 12.5 to 14.5 min isocratic at 90% B, 14.5 to 15.0 min linear to 50% B, and 15.0 to 21.0 min isocratic at 50% B.

MAPK11 and TAK715 were tested in a mixture with six drug molecules to simulate a screening situation. Carbamazepine, norethisterone, warfarin, phenylbutazone, celecoxib, and diclofenac were used as test compounds without p38 $\alpha$  affinity. TAK715 was injected at 20- $\mu\text{M}$  concentration,

the others at 50  $\mu\text{M}$ . The mixture was separated with the following gradient: 0 to 2.0 min isocratic at 50% B, 2.0 to 32.0 min linear to 70% B, 32.0 to 38.0 min isocratic at 70% B, 38.0 to 38.5 min linear to 50% B, and 38.5 to 50.0 min isocratic at 50% B.

For the measurements of  $\text{IC}_{50}$  values, isocratic elution was applied, taking care that the substance peak showed separation from the injection peak. TAK715 was eluted at 85% B, BIRB796 at 50%, and MAPK11 at 70%. Solutions of nine different concentrations for each inhibitor were prepared in 50% methanol, 50% water, and 0.01% formic acid from 5-mM stock solutions of TAK715 and BIRB796 in methanol or a 2-mM stock solution of MAPK11 in DMSO. The following concentrations for each inhibitor were prepared: 50, 100, 200, 500 nM, 1, 2, 5, 10, and 20  $\mu\text{M}$  for TAK715; 500 nM, 1, 2, 5, 10, 20, 50, 100, and 200  $\mu\text{M}$  for BIRB796; and 200, 500 nM, 1, 2, 5, 10, 20, 50, and 100  $\mu\text{M}$  for MAPK11. These nine concentrations and a blank were injected in triplicate for every inhibitor.

To finalize the binding mode studies, the pyrazolourea compound was used as an example of a type III inhibitor. It was injected at a concentration of 100  $\mu\text{M}$  and tested under isocratic conditions at 70% B.

## Results and discussion

### Assay condition optimization

Optimization was carried out in a 96-well format. The protocol of Regan et al. [10] was used with some modifications. Since  $\text{Mg}^{2+}$  ions are known to be involved in ATP binding and can potentially influence binding of inhibitors to the ATP-binding site,  $\text{MgCl}_2$  was added. Furthermore, ELISA blocking reagent and PEG 6000 were added in order to avoid non-specific binding and unwanted interactions with the material of the enzyme binding detection [26]. Enzyme and tracer concentrations were optimized under these conditions. The fluorescence signal showed a linear dependence on the enzyme concentration (cf Online Resource 1 Fig. S1). The most suitable p38 $\alpha$  concentration was therefore chosen by considering the  $Z'$  factor measurements. The signal dependence on the tracer concentration, depicted in Fig. 2a, displays the asymptotic form of saturation behavior. The final concentration of 630 nM SKF is selected to be slightly above the saturation value. This choice presents a compromise between avoiding deviations of the signal due to variability in the tracer concentration and maximizing the sensitivity with regard to detection limits for binders. Namely, competition reduces this sensitivity with increasing tracer concentration.

There are several factors mainly related to the HPLC separation system, which can have a negative influence on

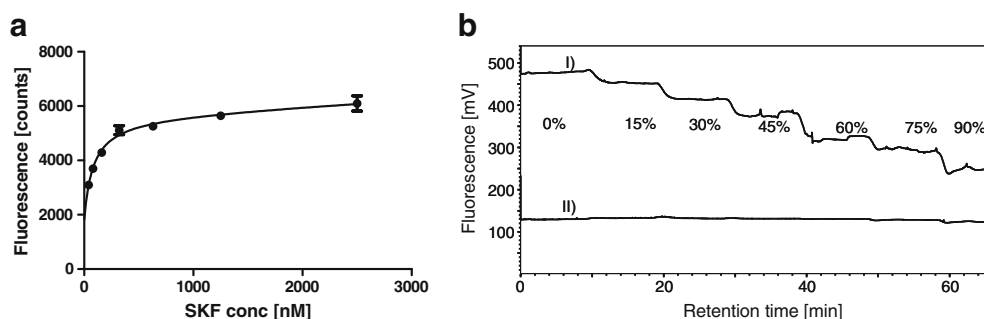


**Fig. 2** Optimization of the p38 $\alpha$  affinity assay. **a** Saturation curve of the tracer for 90 nM p38 $\alpha$  ( $n=3$ ). Full saturation was reached at 630 nM SKF, which was consequently the selected tracer concentration. **b** Influence of the organic modifier concentration on the enzyme binding detection. *I* is the baseline at different percentages of organic modifier in HPLC mobile phase, which shows the maximum signal

reached at these different MeOH concentrations. In opposition, *line II* shows the fluorescence signal at maximum inhibition; hence, the difference between both lines describes the maximum assay window. *II* was measured by premixing SKF with MAPK11 (900 nM final concentration) in the superloop

the assay performance. Methanol, formic acid, and the incubation temperature are the most prominent of these variables. Using typical HPLC conditions such as 50% methanol and 0.1% formic acid at 37 °C completely inhibited the fluorescence enhancement. As a result, these factors were carefully optimized and need to be controlled cautiously. The influence of organic modifier at no and full inhibition is shown in Fig. 2b. The assay window decreased with increasing organic modifier (methanol) content. However, the  $Z'_{\text{chrom}}$  factors for the different compounds measured at different MeOH concentrations, due to gradient elution, showed only minor differences, thereby proving the robustness of the online setup even at high methanol concentrations. Increasing temperature also yielded a similar decrease in maximum signal as seen with methanol. In order to guarantee robustness and enable the use of up to 90% methanol in the HPLC separation, the formic acid concentration in the eluent and the incubation temperature were restricted to 0.01% and 25 °C, respectively. Hence,

the temperatures of the HPLC separation step and the enzyme binding detection were controlled separately.

The screening of highly lipophilic compounds is not only challenging in off-line screening due to adhesion and solubility issues [27] but also presents challenges in online screening approaches [26]. In online screening systems, the amount of organic modifier is usually kept low to prevent protein degradation. On the other hand, the tubing used for incubation loops is mostly PEEK or PTFE. The favored interaction of non-polar compounds with these surfaces results in peak broadening and tailing, thus decreasing resolution and sensitivity. By using polar material for the incubation loops, this effect was significantly decreased. Figure 3a shows a twofold to threefold increase in signal height and reduced tailing when untreated fused silica tubing is used instead of PEEK. Although PTFE compared to PEEK already yields decreased peak width, the width is additionally approximately halved with untreated fused silica. The polarity of the incubation coil material plays a

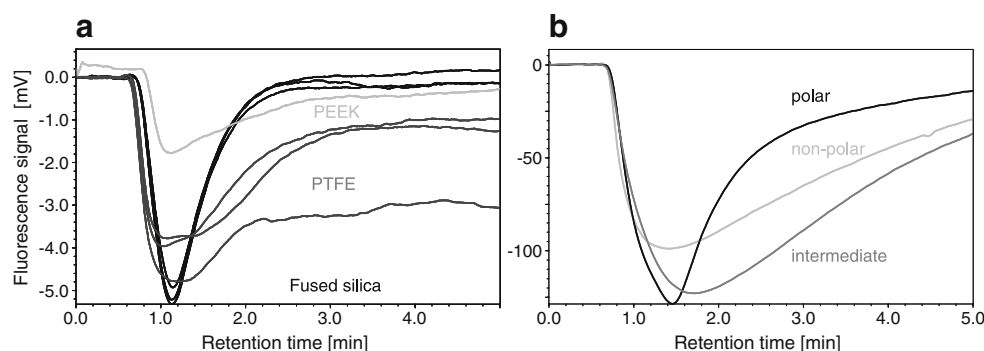


**Fig. 3** Influence of the reaction coil material on the peak shape. **a** PEEK and PTFE were compared with untreated fused silica tubing. A 2- $\mu$ M solution of ORGX was injected in FIA mode at 60% methanol. **b** At the same conditions, a 20- $\mu$ M solution of the same inhibitor was injected. Fused silica tubing with covalent coatings of either PEG (polar), a mixture of methyl and phenyl groups (intermediate), or only

methyl groups (non-polar) was compared for their influence. In both experiments, peak width and asymmetry increased with decreasing polarity while the peak height decreased as a consequence. Fused silica tubing, coated with PEG (polar), exhibited drastically improved performance over the compared materials



crucial role in explaining these findings. This can clearly be seen in Fig. 3b where the influence of fused silica tubing with covalent coatings of different polarities on the peak shape was compared. The polar (PEG-coated) tubing gave the best results while peak height and shape degraded towards intermediate (methyl/phenyl-coated) and non-polar (methyl-coated) surfaces. This indicates the influence of tubing polarity on post-column band broadening and justifies a preference of polar-coated fused silica tubing over PEEK and PTFE in the presented study, taking the structural features of the studied compounds into account.

#### Validation of the p38 $\alpha$ binding assay

The quality of the p38 $\alpha$  binding assay was assessed using the method of Zhang et al. [25]. The  $Z'$  factor is introduced as a single value to judge assay quality because it incorporates the SD of signal and background as well as the assay window. Therefore, it indicates the ability to distinguish between signals and false positives or false negatives. According to this method, the  $Z'$  factor was calculated with Eq. 1 for several enzyme concentrations in the plate-reader-based setup.  $\mu_s$  and  $\mu_c$  are defined as the average signal of the sample and the control, respectively. Consequently,  $\sigma_s$  and  $\sigma_c$  are the standard deviations (SD) of these values.

$$Z' = 1 - \frac{(3\sigma_s + 3\sigma_c)}{|\mu_s - \mu_c|} \quad (1)$$

For the sake of comparability, the number of experiments ( $n=15$ ) was kept the same in plate-reader- and online-based measurements. However, this is recognized as a relatively low number for plate reader experiments. Therefore, an additional plate reader experiment with  $n=50$  was performed, yielding a  $Z'$  factor of  $-0.02$ . The conclusion from both experiments was as follows: the plate-reader-based assay at 90 nM p38 $\alpha$  gave insufficient results with  $Z'$  factors lower than zero. In the plate reader assay, a  $Z'$  factor above 0.5, indicating an excellent assay, could only be achieved by raising the p38 $\alpha$  concentration to 450 nM. Table 1 compares these data with the results of the online setup, in which 90 nM p38 $\alpha$  was sufficient for an excellent assay. As a confirmation, the signal-to-noise ratios (S/N) were also calculated (Table 1), resulting in the same conclusions.

Regardless of the findings of the last paragraph, the online setup has two disadvantages. Reagent consumption is usually higher in an online setup than in a plate-reader-based assay. Furthermore, the separation step introduces an additional dilution due to chromatographic peak broadening, which requires higher analyte concentrations. There are additional differences between the two setups, which

**Table 1**  $Z'$  factors and S/N for plate-reader- and/or online-based enzyme binding detection

	Inhibitor <sup>a</sup>	c (p38 $\alpha$ ) (nM)	$Z'$ or $Z'_{\text{chrom}}$ <sup>b</sup> ( $n=15$ )	S/N
Plate reader	TAK715	90	$-0.41$	4
		180	0.49	12
		270	0.36	23
		360	0.49	55
		450	0.75	48
Online	BIRB796	90	0.77	70
	ORGX	90	0.82	106
	TAK715	90	0.80	97

<sup>a</sup> Concentration of the inhibitor was 1  $\mu\text{M}$  TAK715 (final concentration) in the plate reader experiments. In the online setup, ORGX and TAK715 were injected at 20- $\mu\text{M}$  concentration and BIRB796 at 50  $\mu\text{M}$  concentration for this purpose

<sup>b</sup> In the plate reader experiments, the  $Z'$  factor was calculated according to Eq. 1. For the online experiments, Eq. 2 was used, yielding the  $Z'_{\text{chrom}}$  factor

should be adequately reflected in the  $Z'$  factor. Kool et al. already applied the  $Z'$  factor to chromatography-based online assays, adapting the variables of Eq. 1 in order to take into account these discrepancies [28]. A main advantage is the internal control value ( $\mu_c$ ) represented by the baseline, which is more relevant than an external control, because it is available for each individual experiment. For a complete consideration of the differences between the online and the plate reader setup, all classical variables are systematically substituted with parameters more suitable to the online approach. Doing this without compromising the comparability of this  $Z'$  factor is not trivial but possible. The assay window ( $\mu_c - \mu_s$ ), as determined by the difference of the mean of control (no inhibition) and signal (full inhibition), could more suitably be expressed as the mean of the peak height of full inhibition ( $\mu_H$ ), thereby still describing the desired parameter. Thus, the assay window is automatically corrected for changes in the baseline, representing the internal control. The SD of the sample ( $\sigma_s$ ) would then consequentially be identified with the SD of the peak heights at full inhibition. For the control, usually, no signals are obtained, and changes of the baseline between samples are irrelevant as they have already been taken into account. The SD of the control ( $\sigma_c$ ) can therefore logically be identified with the baseline deviation within one sample. This value is, in chromatography, better known as the noise. The measure of three times the noise is often used as limit of detection. This is consistent with the ideas behind the  $Z'$  factor as both interpretations of  $3\sigma_c$  are aimed at avoiding false positives. In summary, the transition from an external control to an internal one strengthens the reproducibility and accuracy of

the assay and should therefore be appropriately reflected in the determination of  $Z'$  factors. Therefore, an adjusted  $Z'$  factor for the use in online systems is proposed in Eq. 2 on the basis of the previous argumentation.

$$Z'_{\text{chrom}} = 1 - \frac{(3SD_H + 3 \cdot \text{noise})}{|\mu_H|} \quad (2)$$

The new interpretation of the  $Z'$  factor could also be used to omit the measurements of a control, significantly shortening the time of  $Z'_{\text{chrom}}$  factor determination. Because the noise is calculated from the baseline of the chromatogram, a prerequisite is to have an empty time frame to observe both required values. Therefore, the first 4 min of the enzyme binding detection chromatogram was used to determine the noise. The mean noises calculated from signal and control runs were identical, thus proving the redundancy of the control measurements for  $Z'_{\text{chrom}}$  factor determinations.

The repeatability of triplicates is excellent, which is clearly visible in Figs. 4, 5, and 6. This is true for the enzyme binding detection responses as well as for the chromatographic parameters like peak width, measured as full width at half maximum (FWHM), and retention time ( $t_r$ ). For the enzyme binding detection, the relative SDs are  $\leq 10\%$  for FWHM and  $< 3\%$  for  $t_r$ . Low variability and noise compared to the total signal result in the high  $Z'$  factor and S/N shown in Table 1. The high  $Z'$  factors indicate the excellent intraday and interday reproducibility. However,

the online setup showed comparable  $Z'$  factors at five times lower enzyme concentration than needed in the plate-based assay. This is directly related to the minimal measurable  $IC_{50}$ . While  $IC_{50}$  values down to 45 nM can be distinguished in the online method, the plate reader method only allows differentiation of  $IC_{50}$  values of 230 nM and higher. Furthermore, the higher enzyme concentration needed diminishes the advantage of the plate setup with regard to reagent consumption. Therefore, the online setup has advantages beside the additional possibilities associated with separation.

### High-resolution screening of mixtures

In order to assess whether the presented HRS method was suitable for the identification of small-molecule binders of p38 $\alpha$  in mixtures, a solution of eight compounds was screened. Two of these were the kinase inhibitors MAPK11 and TAK715 while the other six were drug molecules from different classes. As illustrated in Fig. 5, all eight compounds could be separated for individual identification and affinity assessment. Based on HR-MS data, the structure was linked to a retention time. Accurate mass measurements enabled the unambiguous distinction of all compounds as two of them differed by less than 0.05 U. In case of more scarce knowledge of the sample, structure elucidation can be facilitated by HR-MS<sup>n</sup> experiments [21]. In parallel to the structure confirmation, the retention time

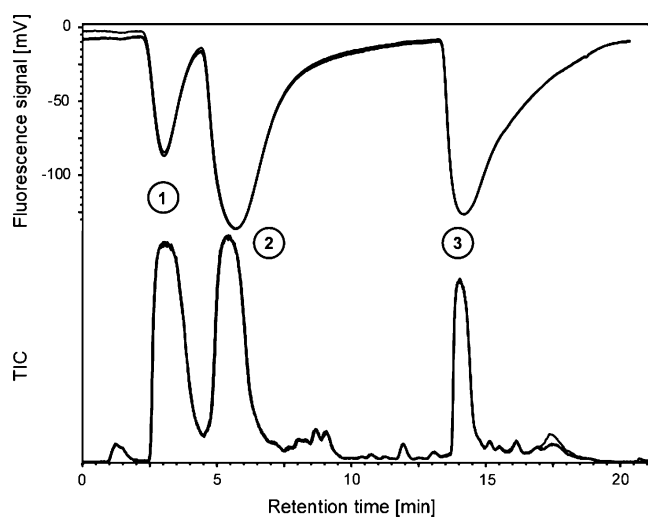


**Fig. 4** Comparison of MS and enzyme binding detection chromatogram. The matching of the fluorescence trace of the enzyme binding detection (*above*) and the total ion current (TIC) of the MS (*below*) for BIRB796 (1), ORGX (2), and TAK715 (3) are shown. Depicted is a triplicate from the  $Z'_{\text{chrom}}$  factor determination. The excellent reproducibility in response, peak shape, and retention time are clearly visible for both the enzyme binding detection and the MS signal. The low variability enables an easy and accurate matching of the two traces

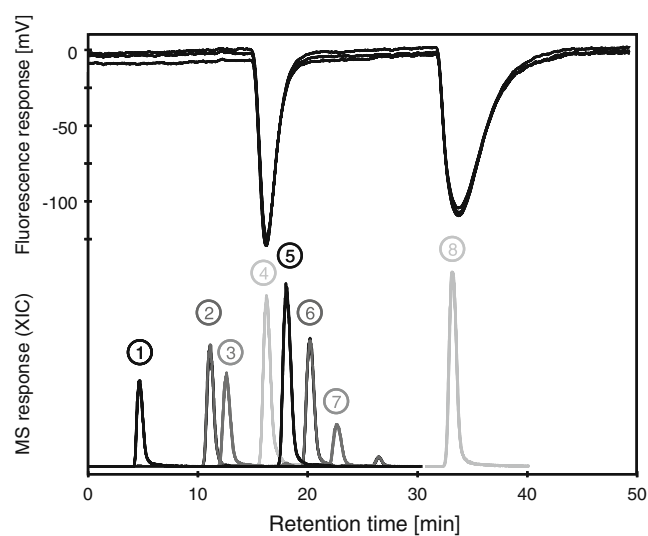


**Fig. 5** HRS of a mixture of kinase inhibitors and drug molecules. MAPK11 (4) and TAK715 (8) were mixed with carbamazepine (1), norethisterone (2), warfarin (3), phenylbutazone (5), celecoxib (6), and diclofenac (7). The mixture was separated by HPLC and measured with HR-MS and enzyme binding detection in parallel. Accurate mass measurements with low deviation ( $< 8$  ppm) and well-matched isotope patterns allowed unambiguous identification. Structure and affinity were easily matched via the corrected retention times. Consequently, the two affinity compounds were detected in the mixture

is also linked with affinity information through the enzyme binding detection. However, the readout of the enzyme binding detection is delayed compared to the HR-MS readout because of a higher void volume and a lower average flow rate after splitting. This delay was measured to be 0.5 min by comparing both detection times in several experiments. It remains constant as long as void volume and flow rates are unchanged. The retention time corrected for this delay is used to couple affinity to identity information. Two affinity peaks were detected, which were linked to the elution of the kinase inhibitors. In conclusion, the approach presents a fast method to match the structure and activity of compounds in mixtures.

### Semi-quantitative affinity measurements

Several known p38 $\alpha$  inhibitors were tested for their dose-related responses in the enzyme binding detection. Therefore, their injected concentrations had to be converted to final assay concentrations by taking into account the dilution factors. On one hand, splitting of the HPLC eluent and subsequent mixing with the reagents led to dilution. This can be easily calculated from the ratios of the flow in the beginning and the end of the enzyme binding detection (113/13=9). On the other hand, the chromatographic dilution, meaning the transition from an injected plug to a series of peaks of (assumed) Gaussian shape, has to be taken into account. The corresponding calculations have been described elsewhere [29]. The necessary peak parameters were taken from the enzyme binding detection. By dividing the injected concentration by the product of both dilution factors, the final concentration at maximum peak height can be calculated and used in the IC<sub>50</sub> calculations (for a brief description, see Online Resource 1).

Dose–response curves depicted in Fig. 6 were measured in triplicate with excellent  $R^2$  values of >0.998 and minimal

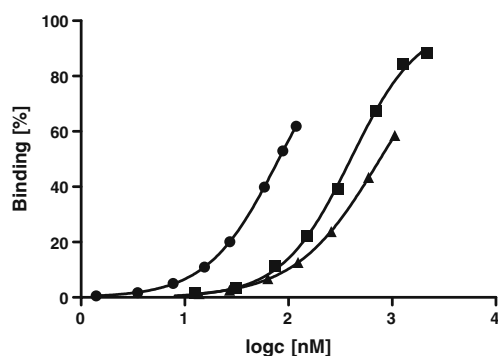


**Fig. 6** Semi-quantitative data of the tested p38 $\alpha$  inhibitors. Binding curves are depicted for several known p38 $\alpha$  inhibitors. The inhibitors TAK715 (circles), BIRB796 (squares), and MAPK11 (triangles) are shown. Standard deviations of triplicate measurements were smaller than data point size

SD of the triplicates (<2% SD relative to assay window). This shows again the excellent reproducibility and accuracy of the assay. The IC<sub>50</sub> values and, given in brackets, their 95% confidence intervals, calculated after correcting the concentrations for the dilution factors, are 81 nM (71 to 92 nM) for TAK715, 400 nM (360 to 440 nM) for BIRB796, and 760 nM (530 to 1,100 nM) for MAPK11. If the inhibitors are ranked for their affinity, the obtained results are in agreement with other methods, stating values of 7.1 nM for TAK715 [8], 18 nM for BIRB796 [10], and 35 nM for MAPK11 [9]. However, the absolute values of measurements are ten to 20 times higher than in literature. This can be explained by the profound differences in the assay formats. While the reported method gives affinities, the reference values were obtained by either activity assays (TAK715) or cell-based functional assays (BIRB796, MAPK11). Another specific reason responsible for this deviation is the slow binding kinetics of BIRB796. This compound is known to show an up to 12-fold deviation of its IC<sub>50</sub> value, depending on the incubation time [11]. Despite the aforementioned issues, the method was proven to be suitable for the semi-quantitative assessment of small-molecule relative affinities towards p38 $\alpha$ , serving as a selection tool in the drug discovery process.

### Applicability and binding modes

The type of binding to p38 $\alpha$  as discussed in the “Introduction” can have a significant influence on the ability of a screening technology to detect this binding. SKF is a type I binder and should therefore enable the detection of type I and type II binders as they compete for the ATP-binding pocket. This has been proven by the

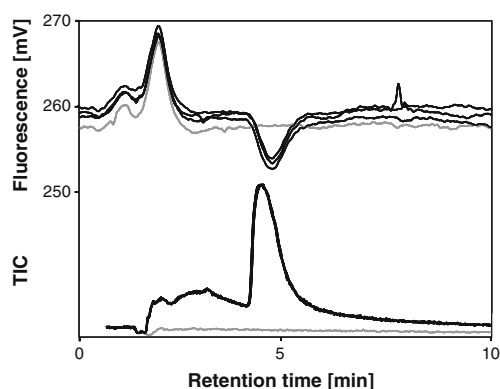


**Fig. 7** Detection of the binding of the pyrazolourea type III inhibitor to p38 $\alpha$ . Triplicate injections of the inhibitor (black) showed signals in the enzyme binding detection (top). In contrast, the control (gray) did not show binding to p38 $\alpha$ . HR-MS (bottom) confirmed the pyrazolourea compound as the binder. This clearly shows the ability of the assay to detect type III inhibitors. In combination with Fig. 4, it proves the applicability to several types of p38 $\alpha$  inhibitors (types I, II, and III)



detection of TAK715 and MAPK11 (type I) as well as BIRB796 (type II). Furthermore, structural changes in p38 $\alpha$  upon binding of type III inhibitors may allow the detection of such compounds. The rearrangement of p38 $\alpha$  from the DFG-in to the DFG-out conformation results in a reorientation of Phe405, thereby affecting the ATP-binding pocket. Hence, we tested the pyrazolourea structure, which was discussed by Simard et al. as an example of a type III inhibitor [12]. Figure 7 shows the enzyme binding detection of this compound to p38 $\alpha$ , thereby proving the suitability of the method for the detection of type III inhibitors. Consequently, the assay is capable of detecting a wide range of p38 $\alpha$  binders including type I, II, and III binders.

## Conclusion

An online binding assay for the separation and parallel assessment of identity and affinity of small molecules in complex mixtures towards non-phosphorylated p38 $\alpha$  was developed. In terms of applicability, the scope of the presented HRS platform is different from conventional HTS assays. HTS is more suited for the screening of huge libraries where speed and low sample consumption are essential. The value of HRS lies in the parallel determination of structural and biochemical data of potential binders. While an HTS assay will only give a sum of compound affinities, HRS gives individual information on all (separated) molecules. The aim was to make available the advantages of the online approach, mainly the measurement of mixtures and a comparison of structure and affinity, for the important drug target p38 $\alpha$ . An online post-column enzyme binding detection based on fluorescence enhancement was developed, and its compatibility with modern HPLC separation techniques, such as gradient elution and increased temperature, was demonstrated. HR-MS as parallel readout is an integral part of the developed screening platform, allowing the identification of the tested molecules. Additionally, the prospects of measuring compounds individually in mixtures were demonstrated by matching identity and affinity. Regarding the presented assay validation data, it can be stated that a high-quality assay was achieved. Finally, the assay provided ranking of various p38 $\alpha$  inhibitors (types I, II, and III), allowing the use within a drug discovery process.

**Acknowledgements** This work was performed within the framework of the Dutch Top Institute Pharma project D2-102. We thank MSD research laboratories for kindly providing p38 $\alpha$  and other chemicals. We thank Guido Zaman for important discussions. The work of the author M. Giera was supported by the German Academic Exchange Service (DAAD).

**Open Access** This article is distributed under the terms of the Creative Commons Attribution Noncommercial License which permits any noncommercial use, distribution, and reproduction in any medium, provided the original author(s) and source are credited.

## References

- Cohen P (2002) Protein kinases—the major drug targets of the twenty-first century? *Nat Rev Drug Discov* 1(4):309–315
- Zhang J, Shen B, Lin A (2007) Novel strategies for inhibition of the p38 mapk pathway. *Trends Pharmacol Sci* 28(6):286–295
- Kumar S, Boehm J, Lee JC (2003) P38 map kinases: key signalling molecules as therapeutic targets for inflammatory diseases. *Nat Rev Drug Discov* 2(9):717–726
- Saklatvala J (2004) The p38 map kinase pathway as a therapeutic target in inflammatory disease. *Curr Opin Pharmacol* 4(4):372–377
- Schindler JF, Monahan JB, Smith WG (2007) P38 pathway kinases as anti-inflammatory drug targets. *J Dent Res* 86(9):800–811
- Mayer RJ, Callahan JF (2006) P38 map kinase inhibitors: a future therapy for inflammatory diseases. *Drug Discov Today* 3(1):49–54
- Goldstein DM, Kuglstat A, Lou Y, Soth MJ (2010) Selective p38alpha inhibitors clinically evaluated for the treatment of chronic inflammatory disorders. *J Med Chem* 53(6):2345–2353
- Miwatashi S, Arikawa Y, Kotani E, Miyamoto M, Naruo K, Kimura H, Tanaka T, Asahi S, Ohkawa S (2005) Novel inhibitor of p38 map kinase as an anti-tnf-alpha drug: discovery of *n*-[4-[2-ethyl-4-(3-methylphenyl)-1,3-thiazol-5-yl]-2-pyridyl]benzamide (tak-715) as a potent and orally active anti-rheumatoid arthritis agent. *J Med Chem* 48(19):5966–5979
- de Laszlo SE, Visco D, Agarwal L, Chang L, Chin J, Croft G, Forsyth A, Fletcher D, Frantz B, Hacker C, Hanlon W, Harper C, Kostura M, Li B, Luell S, MacCoss M, Mantlo N, O'Neill EA, Orevillo C, Pang M, Parsons J, Rolando A, Sahly Y, Sidler K, O'Keefe SJ (1998) Pyrroles and other heterocycles as inhibitors of p38 kinase. *Bioorg Med Chem Lett* 8(19):2689–2694
- Regan J, Breitfelder S, Cirillo P, Gilmore T, Graham AG, Hickey E, Klaus B, Madwed J, Moriaki M, Moss N, Pargellis C, Pav S, Proto A, Swinamer A, Tong L, Torcellini C (2002) Pyrazole urea-based inhibitors of p38 map kinase: from lead compound to clinical candidate. *J Med Chem* 45(14):2994–3008
- Pargellis C, Tong L, Churchill L, Cirillo PF, Gilmore T, Graham AG, Grob PM, Hickey ER, Moss N, Pav S, Regan J (2002) Inhibition of p38 map kinase by utilizing a novel allosteric binding site. *Nat Struct Biol* 9(4):268–272
- Simard JR, Klüter S, Grütter C, Getlik M, Rabiller M, Rode HB, Rauh D (2009) A new screening assay for allosteric inhibitors of CSRC. *Nat Chem Biol* 5(6):394–396
- Adrian FJ, Ding Q, Sim T, Velentza A, Sloan C, Liu Y, Zhang G, Hur W, Ding S, Manley P, Mestan J, Fabbro D, Gray NS (2006) Allosteric inhibitors of bcr-abl-dependent cell proliferation. *Nat Chem Biol* 2(2):95–102
- Klump M, Boettcher A, Becker D, Meder G, Blank J, Leder L, Forstner M, Ottl J, Mayr LM (2006) Readout technologies for highly miniaturized kinase assays applicable to high-throughput screening in a 1536-well format. *J Biomol Screen* 11(6):617–633
- Olive DM (2004) Quantitative methods for the analysis of protein phosphorylation in drug development. *Expert Rev Proteomics* 1(3):327–341
- Zaman GJ, van der Lee MM, Kok JJ, Nelissen RL, Loomans EE (2006) Enzyme fragment complementation binding assay for p38alpha mitogen-activated protein kinase to study the binding kinetics of enzyme inhibitors. *Assay Drug Dev Technol* 4(4):411–420

17. Lee JC, Laydon JT, McDonnell PC, Gallagher TF, Kumar S, Green D, McNulty D, Blumenthal MJ, Heys JR, Landvatter SW, Strickler JE, McLaughlin MM, Siemens IR, Fisher SM, Livi GP, White JR, Adams JL, Young PR (1994) A protein kinase involved in the regulation of inflammatory cytokine biosynthesis. *Nature* 372(6508):739–746
18. Munoz L, Selig R, Yeung YT, Peifer C, Hauser D, Laufer S (2010) Fluorescence polarization binding assay to develop inhibitors of inactive p38alpha mitogen-activated protein kinase. *Anal Biochem* 401(1):125–133
19. Young PR, McLaughlin MM, Kumar S, Kassis S, Doyle ML, McNulty D, Gallagher TF, Fisher S, McDonnell PC, Carr SA, Huddleston MJ, Seibel G, Porter TG, Livi GP, Adams JL, Lee JC (1997) Pyridinyl imidazole inhibitors of p38 mitogen-activated protein kinase bind in the ATP site. *J Biol Chem* 272(18):12116–12121
20. de Vlieger JS, Kolkman AJ, Ampt KA, Commandeur JN, Vermeulen NP, Kool J, Wijmenga SS, Niessen WM, Irth H, Honing M (2010) Determination and identification of estrogenic compounds generated with biosynthetic enzymes using hyphenated screening assays, high resolution mass spectrometry and off-line NMR. *J Chromatogr B* 878(7–8):667–674
21. Giera M, de Vlieger JS, Lingeman H, Irth H, Niessen WM (2010) Structural elucidation of biologically active neomycin *n*-octyl derivatives in a regioisomeric mixture by means of liquid chromatography/ion trap time-of-flight mass spectrometry. *Rapid Commun Mass Spectrom* 24(10):1439–1446
22. Van Liempd SM, Kool J, Meerman JH, Irth H, Vermeulen NP (2007) Metabolic profiling of endocrine-disrupting compounds by on-line cytochrome p450 bioreaction coupled to on-line receptor affinity screening. *Chem Res Toxicol* 20(12):1825–1832
23. Giera M, Heus F, Janssen L, Kool J, Lingeman H, Irth H (2009) Microfractionation revisited: a 1536 well high resolution screening assay. *Anal Chem* 81(13):5460–5466
24. Shi SY, Zhou HH, Zhang YP, Jiang XY, Chen XQ, Huang KL (2009) Coupling HPLC to on-line, post-column (bio)chemical assays for high-resolution screening of bioactive compounds from complex mixtures. *Trends Anal Chem* 28(7):865–877
25. Zhang JH, Chung TD, Oldenburg KR (1999) A simple statistical parameter for use in evaluation and validation of high throughput screening assays. *J Biomol Screen* 4(2):67–73
26. Kool J, van Liempd SM, Ramautar R, Schenk T, Meerman JH, Irth H, Commandeur JN, Vermeulen NP (2005) Development of a novel cytochrome p450 bioaffinity detection system coupled online to gradient reversed-phase high-performance liquid chromatography. *J Biomol Screen* 10(5):427–436
27. Schebb NH, Falck D, Faber H, Hein EM, Karst U, Hayen H (2009) Fast method for monitoring phospholipase a2 activity by liquid chromatography–electrospray ionization mass spectrometry. *J Chromatogr A* 1216(27):5249–5255
28. Kool J, van Marle A, Hulscher S, Selman M, van Iperen DJ, van Altena K, Gillard M, Bakker RA, Irth H, Leurs R, Vermeulen NP (2007) A flow-through fluorescence polarization detection system for measuring GPCR-mediated modulation of camp production. *J Biomol Screen* 12(8):1074–1083
29. Schebb NH, Heus F, Saenger T, Karst U, Irth H, Kool J (2008) Development of a countergradient parking system for gradient liquid chromatography with online biochemical detection of serine protease inhibitors. *Anal Chem* 80(17):6764–6772